

Room-temperature fabrication of light-emitting thin films based on amorphous oxide semiconductor

Cite as: AIP Advances 6, 015106 (2016); <https://doi.org/10.1063/1.4939939>

Submitted: 13 December 2015 • Accepted: 04 January 2016 • Published Online: 11 January 2016

 Junghwan Kim, Norihiko Miyokawa, Keisuke Ide, et al.



View Online



Export Citation



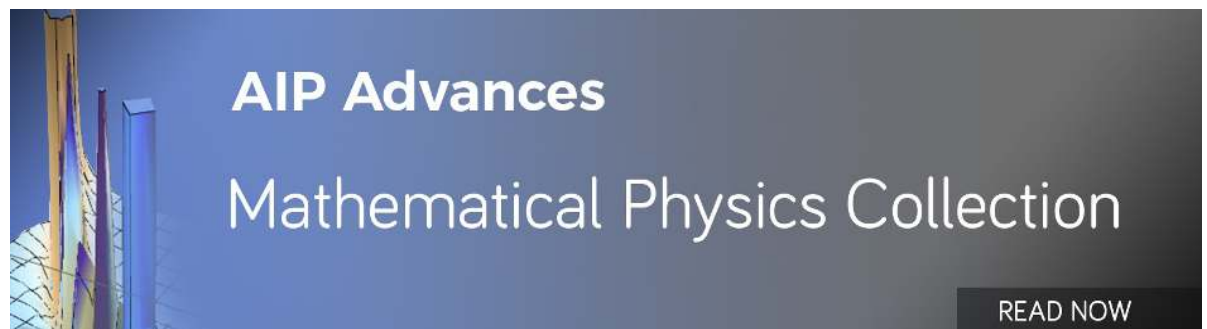
CrossMark

ARTICLES YOU MAY BE INTERESTED IN

[Ultra-wide bandgap amorphous oxide semiconductors for NBIS-free thin-film transistors](#)
APL Materials **7**, 022501 (2019); <https://doi.org/10.1063/1.5053762>

[Performance boosting strategy for perovskite light-emitting diodes](#)
Applied Physics Reviews **6**, 031402 (2019); <https://doi.org/10.1063/1.5098871>

[Hydrogen anion and subgap states in amorphous In-Ga-Zn-O thin films for TFT applications](#)
Applied Physics Letters **110**, 232105 (2017); <https://doi.org/10.1063/1.4985627>



Room-temperature fabrication of light-emitting thin films based on amorphous oxide semiconductor

Junghwan Kim,^{1,a} Norihiko Miyokawa,¹ Keisuke Ide,¹ Yoshitake Toda,²
Hidenori Hiramatsu,^{1,2} Hideo Hosono,^{1,2} and Toshio Kamiya^{1,2}

¹Materials and Structures Laboratory, Tokyo Institute of Technology, Mailbox R3-4,
4259 Nagatsuta, Midori-ku, Yokohama, Japan

²Materials Research Center for Element Strategy, Tokyo Institute of Technology,
Mailbox SE-6, 4259 Nagatsuta, Midori-ku, Yokohama, Japan

(Received 13 December 2015; accepted 4 January 2016; published online 11 January 2016)

We propose a light-emitting thin film using an amorphous oxide semiconductor (AOS) because AOS has low defect density even fabricated at room temperature. Eu-doped amorphous In-Ga-Zn-O thin films fabricated at room temperature emitted intense red emission at 614 nm. It is achieved by precise control of oxygen pressure so as to suppress oxygen-deficiency/excess-related defects and free carriers. An electronic structure model is proposed, suggesting that non-radiative process is enhanced mainly by defects near the excited states. AOS would be a promising host for a thin film phosphor applicable to flexible displays as well as to light-emitting transistors. © 2016 Author(s). All article content, except where otherwise noted, is licensed under a Creative Commons Attribution (CC BY) license (<http://creativecommons.org/licenses/by/4.0/>). [<http://dx.doi.org/10.1063/1.4939939>]

Most of current flat-panel displays (FPDs) are manufactured at lower temperatures than 400°C, below the strain points of large-size mother glass substrates.¹ Recently, they require a further lower-temperature process for flexible applications using plastic substrates. Currently, organic light-emitting diodes (OLEDs) are the most promising candidate to realize the flexible applications.² However, OLEDs still have several issues, e.g., chemical instability in an ambient environment and short lifetime, which originate largely from the intrinsic nature of organic materials. Further, it is difficult to apply conventional photolithography to organic multilayer structures such as employed in OLEDs; therefore, fine metal masks are used to define pixels in the current RGB-type OLEDs,² which in turn limits large-size production of high-resolution OLEDs.³ These issues arising from nature of organic materials are absent in inorganic LEDs (ILEDs) such as GaN LEDs, but they require single-crystalline substrates and high-temperature processes.⁴

Thus, we consider that these issues would be overcome if we develop new inorganic light-emitting thin films that can be grown at low temperatures. To produce good phosphors, a high temperature process is, in general, required in order to reduce non-radiative recombination centers via defects / strain and to activate emission centers. It is also considered that a host material of a phosphor should be insulating because e.g. energy-back transfer via mobile carriers enhances non-radiative recombination. A host should also have a wide band gap so that it transmits the emitted light. Further, inorganic thin film phosphors targeted at ILEDs must satisfy the additional requirements such as a low temperature process (e.g., < 400°C, and preferably at room temperature) and controlled carrier conduction. The solubility of active center dopants is, in general, limited in crystalline phosphors.⁵ In terms of the process temperature and the solubility limit, an amorphous thin film phosphor appears more advantageous than polycrystalline ones. There have, however, been a limited number of reports on inorganic thin film phosphors including (Y, Eu)Ca₄O(BO₃)₃,⁶ ZnS:(Cu,Al),⁷ etc.,⁸⁻¹⁰ all of which are polycrystalline materials and require rather high process

^aCorresponding author: Junghwan Kim Tel: +81-45-924-5628 Fax: +81-45-924-5350 E-Mail: JH.KIM@lucid.msl.titech.ac.jp

temperatures >500 °C. In particular, using an amorphous thin film as a host would be more challenging because it was believed that amorphous materials have high-density defects. On the other hand, the development of amorphous oxide semiconductor (AOS) thin-film transistors (TFTs) demonstrated that AOSs have low defect densities even fabricated at room temperature.^{11–13} If we choose an active ion that has the relevant emission level well higher than those of the defects, we can expect high-efficiency light-emission by suppressing non-radiative recombination.

We here propose AOS-based thin film phosphors because AOSs satisfy the above requirements such as high transparency, low process temperatures, and low defect density as well as other advantages such as good uniformity and a wide controllability of carrier density.^{11–14} We succeeded in fabricating light-emitting thin films by combining a representative AOS, a-In-Ga-Zn-O, as a host material with Eu as an active center (a-IGZO:Eu_x, x denotes the Eu content at the In site) at room temperature. It was found that oxygen partial pressure during deposition (P_{O_2}) should be tuned to obtain light-emitting thin films because low P_{O_2} generates defects and mobile carriers while high P_{O_2} would introduce excess oxygen-related defects.

All thin films were fabricated by pulsed laser deposition (PLD) using a KrF excimer laser (wavelength: 248 nm) in an O₂ gas flow at room temperature on silica glass substrates without any post-deposition treatment. (In_{1-x}Eu_x)GaZnO₄ polycrystalline ceramic targets were prepared from mixed powders of In₂O₃ (purity, 99.999%), Eu₂O₃ (purity, 99.99%), Ga₂O₃ (purity, 99.99%) and ZnO (purity, 99.999%), which were sintered at 1400 °C for 5 hours in air. Basic deposition parameters were the laser power of 1.5 J/cm² and the target–substrate distance of 40 mm. P_{O_2} was varied from 1 to 7 Pa. Film structures and thickness were characterized and determined by high-resolution X-ray diffraction (HR-XRD) and grazing-incidence X-ray reflectivity (GIXRR), respectively. X-ray diffraction confirmed that all the films were amorphous independent of Eu content and P_{O_2} (data not shown). Photoluminescence / excitation (PL / PLE) spectra were measured at room temperature with a conventional spectrophotometer and fluorescence spectrometer, respectively. Film thickness were adjusted to ~ 120 nm so that we can directly compare the measured PL intensities. Electrical properties were measured by Hall effect with the van der Pauw configuration. Hard X-ray photoemission spectroscopy (HAXPES) measurements were performed at the BL15XU undulator beamline (excitation X-ray energy: $h\nu = 5950.05$ eV) in SPring-8.¹⁵ X-ray absorption spectroscopy (XAS) and resonant photoemission spectroscopy (RPES) measurements were performed at an undulator beamline of BL2C in the Photon Factory, KEK. All the spectra were recorded at 300 K.

As will be explained later, strong PL were observed in a-IGZO:Eu_x films deposited at room temperature when the (In_{2-x}Eu_x)GaZnO₄ target with $x = 0.3$ was used and the deposition condition was optimized to $P_{O_2} = 5$ Pa. Figure 1(a) shows PL and PLE spectra of a-IGZO:Eu_{0.3} films. Clear line emissions assigned to the ⁵D₀ → ⁷F_{*J*} transitions ($J = 0, 1, 2, \dots$) in Eu³⁺ were observed; e.g., at 578 nm for ⁵D₀ → ⁷F₀, 590 nm for ⁵D₀ → ⁷F₁, 614 nm for ⁵D₀ → ⁷F₂, 652 nm for ⁵D₀ → ⁷F₃, and 703 nm for ⁵D₀ → ⁷F₄.^{6,16,17} The strongest emission was the ⁵D₀ → ⁷F₂ electric dipole transition at 614 nm. On the other hand, PLE spectra of the 614 nm emission exhibited a broad band centered at 270 nm (4.59 eV), which is known to be a charge-transfer (CT) process.^{16,17} As shown in Fig. 1(b), we observed intense red emission from the room-temperature fabricated a-IGZO:Eu_{0.3} thin films under 270 nm monochromated light illumination.

Here, we discuss required deposition conditions to produce light-emitting thin films at room temperature. As seen in Fig. 2(a), PL intensity increased linearly with Eu content x and took maximum when x reaches 0.3, and then decreased at higher x . The decrease in PL at $x \geq 0.4$ would be attributed to concentration quenching. Figure 2(b) shows that emission lifetime was almost unchanged at 0.94 ms up to $x = 0.15$, while started decreasing to 0.77 ms for $x = 0.30$, and then rapidly decreased to 0.32 ms for $x = 0.40$. Therefore, it can be concluded that concentration quenching occurred from $x \sim 0.3$, resulting in the significant PL degradation at $x \geq 0.4$, similar to the case reported in Ref. 6 (maximum intensity was reported to be $x = 0.2$ in (Y_{1-x}Eu_x)Ca₄O(BO₃)₃). Hereafter, we discuss on the films with the optimum $x = 0.3$.

Also, we like to point out that P_{O_2} should be tuned to obtain light-emitting films at room temperature. As shown in Fig. 3(a), only very weak PL was detected for the film deposited at a low $P_{O_2} = 1$ Pa, while the most intense PL was obtained at $P_{O_2} = 5$ –6 Pa. Then, PL intensity decreased at further higher P_{O_2} . To clarify these reasons, we performed Hall and optical measurements.

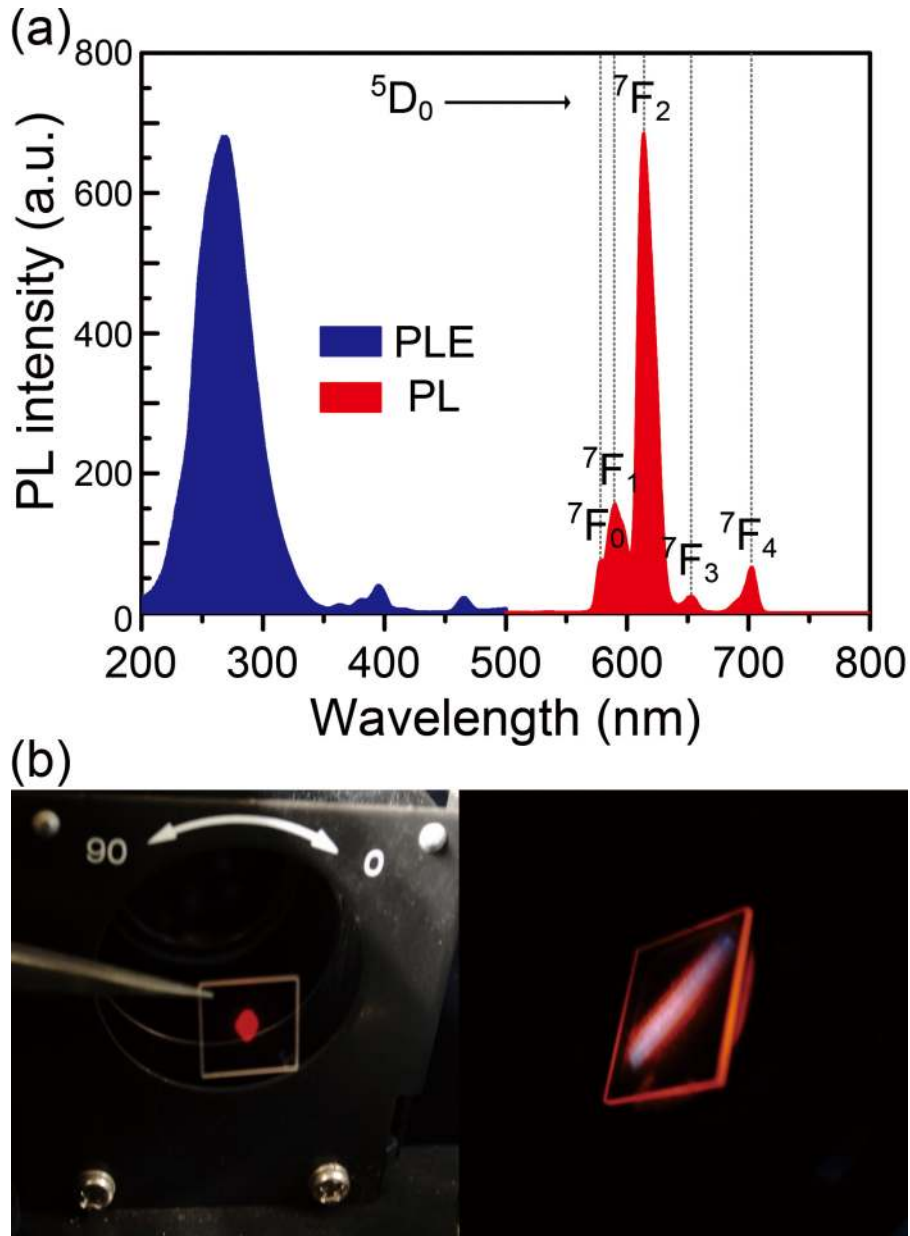


FIG. 1. PL at 300 K from unannealed a-IGZO:Eu_{0.3} thin films deposited at $P_{O_2} = 5$ Pa. (a) PL (excited by monochromated 270 nm light from a fluorescence spectrometer) and PLE spectra (measured at 614 nm). (b) Photos of PL in the fluorescence spectrometer.

Figure 3(a) also shows that free carrier density was somewhat high $>10^{14}$ cm⁻³ for $P_{O_2} = 1$ Pa, and then decreased to 10^{12} cm⁻³ with the increase in P_{O_2} to 6 Pa (note that reliable data were not obtained for higher P_{O_2}), which accompanies the increase in the PL intensity. Optical absorption spectra in Fig. 3(b) show that the fundamental band gap estimated by Tauc' plot was $E_g = 3.4$ eV independent of P_{O_2} , while the subgap absorption (i.e., photon energies $< E_g$) increases with the decrease in P_{O_2} , which would be induced by defects formed due to oxygen deficiencies.¹⁸ HAXPES results further support these results. Figure 3(c) shows that the valence band maximum (VBM) level with respect to the Fermi level ($E_F - E_{VBM}$) decreased with the increase in P_{O_2} as corresponding to the decrease in the carrier density. Furthermore, the density of the defect states observed above E_{VBM} (detected at 1–3 eV in Fig. 3(d)) was obviously higher for $P_{O_2} = 1$ Pa than the higher P_{O_2}

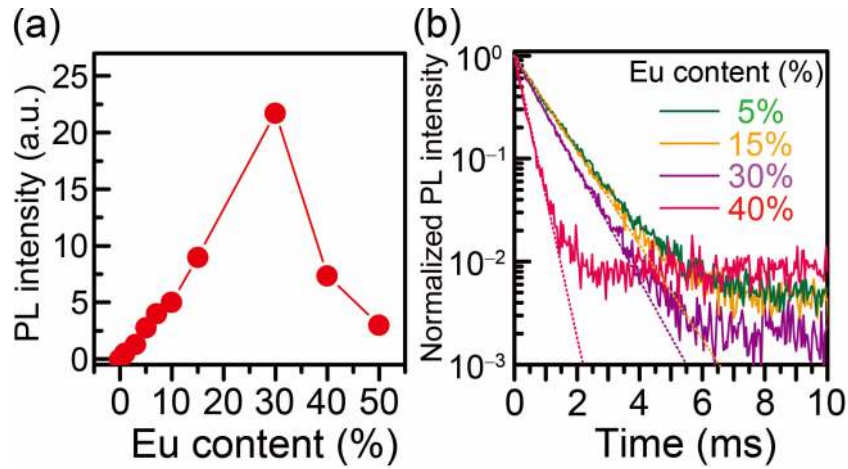


FIG. 2. (a) PL intensity and (b) lifetime as a function of Eu content x for unannealed a-IGZO:Eu $_x$ thin films deposited at $P_{O_2} = 5$ Pa.

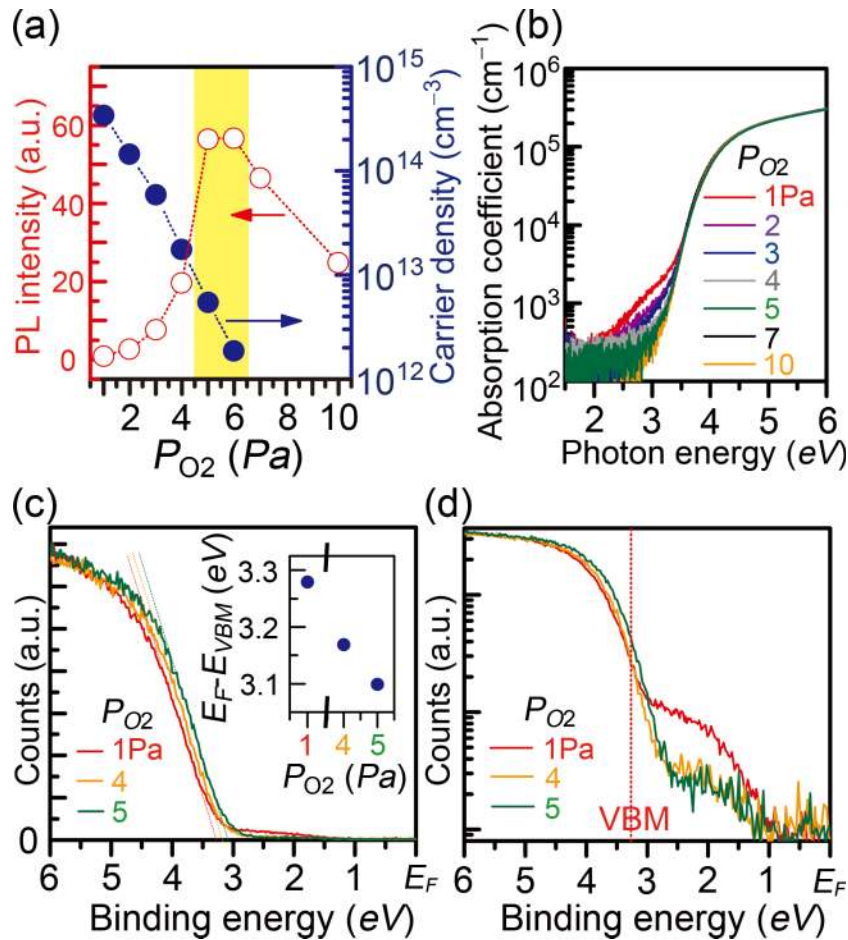


FIG. 3. Effects of P_{O_2} . (a) Relationship between PL intensity (closed symbol) and carrier density (open symbol). (b) Optical absorption spectra. (c,d) Valence band HAXPES spectra plotted in (c) linear scale and (d) logarithmic scale. Binding energy is measured from the Fermi level (E_F). Inset to (c) shows $E_F - E_{VBM}$ as a function of P_{O_2} .

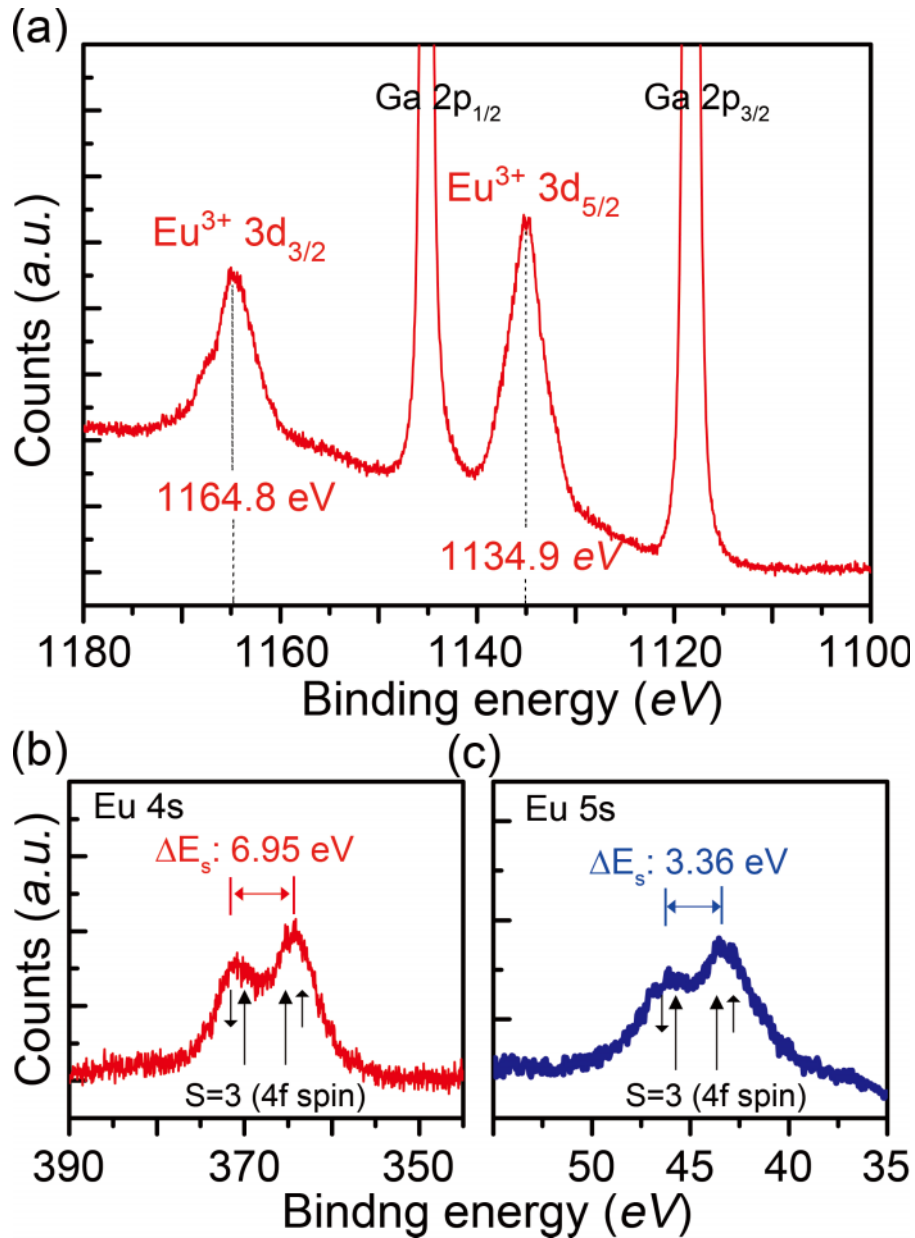


FIG. 4. HAXPES core spectra for (a) Eu 3d, (b) Eu 4s, and (c) Eu 5s.

films. These results imply that non-radiative recombination processes are enhanced in the lower P_{O_2} films, which would be attributed to energy-back transfer via the free carriers as well as energy transfer from excited carriers to the subgap states similar to Auger recombination.

However, PL intensity was deteriorated in the higher P_{O_2} (>6 Pa) films although the free carrier concentrations are further lower (lower than the measurement limit of our apparatus) and the subgap optical absorption did not change anymore. It is reported that if too strong oxidation condition is employed to fabricate a-IGZO films, carrier concentration is decreased but TFT characteristics are deteriorated, which is attributed to defect states formed due to excess/weakly-bonded oxygens (O_{ex}).¹⁹ We consider that also for the a-IGZO: Eu_x case, the O_{ex} -related defects enhanced non-radiative recombination and resulted in the PL intensity degradation at $P_{\text{O}_2} > 6 \text{ Pa}$.

Here, we like to discuss the valence states of the Eu emission centers. It has been reported that Eu-doped phosphors often include mixed-valence states of Eu.^{5,16,20} Suzuki and co-workers

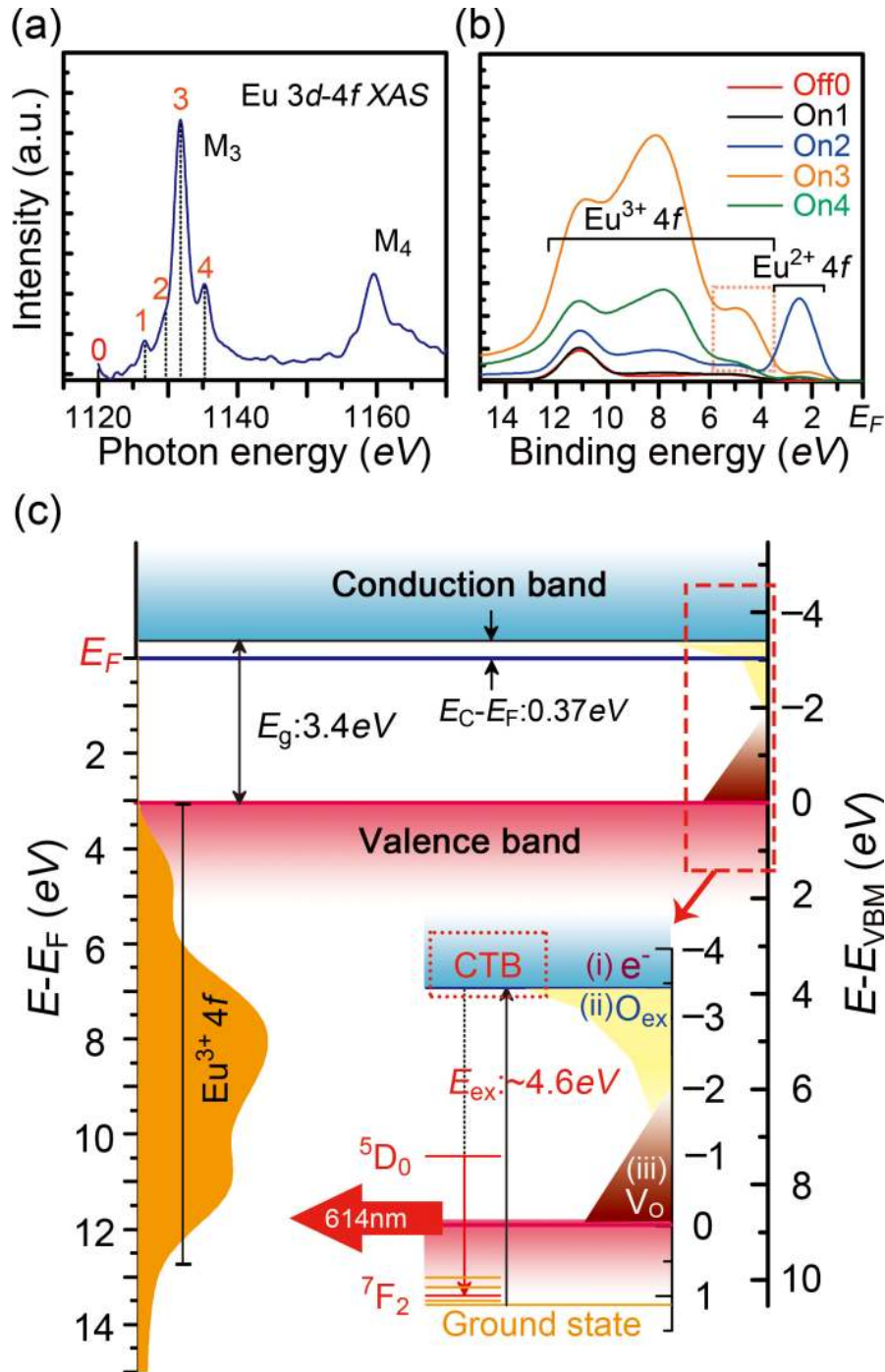


FIG. 5. (a) Eu 3d-4f XAS spectrum. (b) RPES spectra excited by different energies determined from (a); i.e., off0, on1, on2, on3, and on4 for 1120, 1129.5, 1131.8, and 1135.3 eV, respectively as shown in (a) by corresponding numbers. (c) Energy level diagram of a-IGZO:Eu_{0.3}, where two energy axes measured from (left) E_F and (right) E_{VBM} are shown. Inset describes excitation and luminescence processes. The cyan, yellow, and brown regions illustrate (i) free carriers, (ii) excess oxygen traps (O_{ex}), and (iii) oxygen-vacancy defects (V_O), respectively.

report that the degradation of PL is attributed to reduction of trivalent Eu ions ($Eu^{3+} \rightarrow Eu^0$).⁵ Figure 4(a) shows a HAXPES core spectrum of an a-IGZO:Eu_{0.3} film for Eu 3d. Eu-related peaks were observed at ~ 1135 and ~ 1165 eV, which correspond to $Eu^{3+} 3d_{5/2}$ and $3d_{3/2}$, respectively.^{5,20} While, multiplet splitting were observed also for Eu 4s and 5s (Figs. 4(b), 4(c)). The splits of the

ns core levels are attributed to the interaction between the *s* shell and the partially filled 4*f* shell.²¹ The energy splitting were 6.95 and 3.36 eV for Eu 4*s* and 5*s*, respectively, which agree well with theoretical values for trivalent Eu model (6.95 and 3.34 eV, respectively).²¹ The HAXPES results substantiate that all Eu ions incorporated in the a-IGZO:Eu_{0.3} films stably exist as trivalent ions, and which also explain the intense red emission.

Lastly, we investigated the electronic structure of a-IGZO:Eu_{0.3} by RPES. Although RPES spectrum of Eu in an oxide has rarely been reported due to a charging effect,²² reliable XAS and RPES data were obtained for a-IGZO:Eu_{0.3} owing to the semiconducting properties of the film. Eu 3*d*-4*f* XAS spectrum in Fig. 5(a) shows several peak features. Figure 5(b) shows RPES spectra for excitation energies chosen from these peaks (1120, 1129.5, 1131.8, and 1135.3 eV, corresponding to off0, on1, on2, on3, and on4, respectively).²³ Resonantly enhanced PES peaks were observed at ~2.5 eV and in the 3 – 13 eV range, which are attributed to Eu²⁺ and Eu³⁺ 4*f* states, respectively.²³ Although the Eu²⁺ 4*f* states were not detected by the HAXPES spectra (Fig. 4), it would be explained by surface valence transition model.²⁴

Figure 5(c) illustrates the energy levels in a-IGZO:Eu_{0.3} deduced from these data. As discussed in Fig. 1, excitation energy (E_{ex}) for PL centered at 4.59 eV. The excitation mechanism for Eu³⁺ ions has been explained by a CT process,^{16,17} which is consistent with our observation of the CT band (CTB) in the PLE spectrum. As illustrated in the energy level diagram, the highest occupied state of Eu³⁺ 4*f* is around 1 eV below the E_{VBM} . Assuming that these Eu³⁺ 4*f* states are the initial states, the excited states (i.e., CTB) locate near the CBM above the E_{F} . Here, we like to discuss the correlation between the excited states and the defect states. As reported in Ref. 19 for a-IGZO, the O_{ex} -related defects distribute in the near CBM region and are relaxed to very deep levels ~2.3 eV below the CBM upon capture an electron. It indicates that the charge transfer from the excited state to the O_{ex} -related state occurs effectively due to similar energies, and the charge transfer relaxes the O_{ex} -related state to the deep level even closer to E_{VBM} ; thus, the non-radiative process would be much enhanced when O_{ex} -related states are formed. As discussed above, PL is also deteriorated by free carriers in CB. From these results, we expect that light-emitting AOS films will be further improved by designing these defect states, the excited states, and the initial states of the active centers given in this energy diagram.

In summary, we succeeded in fabricating light-emitting a-IGZO:Eu thin films at room temperature. As non-radiative process in the AOS-based thin film phosphor originates from oxygen-deficiency-related defects and consequent free electron generation, appropriate P_{O_2} lead to intense light emission without any thermal annealing. It should also be important to point out that too high P_{O_2} would introduce other defects such as excess/weakly-bonded oxygen; consequently, optimizing deposition condition such as P_{O_2} can produce light-emitting thin films even at room temperature. Further, we built an energy level diagram of the AOS host, the Eu³⁺ ions, and the defect states to explain the excitation and the luminescence processes, which will help to design improved light-emitting films based on AOSs.

This achievement extends applications of AOS to thin-film phosphors fabricable on plastic substrates, leading to all-inorganic LED flexible displays. As the carrier density in AOS can be altered in a wide range also by electric field, electrical-optical coupling devices would also be expected.

ACKNOWLEDGEMENTS

We thank Dr S. Ueda at National Institute for Materials Science (NIMS) and Dr H. Kumigashira at high energy accelerator research organization (KEK) for their assistances of HAXPES and RPES measurements, respectively. This work was supported by the Ministry of Education, Culture, Sports, Science and Technology (MEXT) though Element Strategy Initiative to Form Core Research Center. J. Kim was supported by ACCEL Project sponsored by Japan Science and Technology Agency (JST). H. Hiramatsu was also supported by the Japan Society for the Promotion of Science (JSPS) through a Grant-in-Aid for Scientific Research on Innovative Areas “Nano Informatics” Grant Number 25106007, and Support for Tokyotech Advanced Research (STAR).

- ¹ H. Kim, J. Jeong, H. Chung, and Y. Mo, *SID Symposium Digest of Technical Papers* **39**, 291 (2008).
- ² D. Jin, J. Lee, T. Kim, S. An, D. Straykhilev, Y. Pyo, H. Kim, D. Lee, Y. Mo, H. Kim, and H. Chung, *SID Symposium Digest of Technical Papers* **40**, 983 (2009).
- ³ S. Lee, M. Suh, T. Kang, Y. Kwon, J. Lee, H. Kim, and H. Chung, *SID Symposium Digest of Technical Papers* **38**, 1588 (2007).
- ⁴ S. Nakamura, T. Mukai, and M. Senoh, *Appl. Phys. Lett.* **64**, 1687 (1994).
- ⁵ K. Suzuki, K. Murayama, and N. Tanaka, *Appl. Phys. Lett.* **107**, 031902 (2015).
- ⁶ H. Sano, T. Matsumoto, Y. Matsumoto, and H. Koinuma, *Appl. Phys. Lett.* **86**, 021104 (2005).
- ⁷ J. Kim, H. Hiramatsu, H. Hosono, and T. Kamiya, *Thin Solid Films* **18**, 559 (2014).
- ⁸ S. Yi, J. Bae, B. Moon, J. Jeong, J. Park, and I. Kim, *Appl. Phys. Lett.* **81**, 3344 (2002).
- ⁹ Y. Masuda, M. Yamagashi, and K. Koumoto, *Chem. Mater.* **19**, 1002 (2007).
- ¹⁰ H. Takashima, K. Shimada, N. Miura, T. Katsumata, Y. Inaguma, K. Ueda, and M. Itoh, *Adv. Mater.* **21**, 3699 (2009).
- ¹¹ H. Hosono, *J. Non-Cryst. Sol.* **352**, 851 (2006).
- ¹² K. Nomura, H. Ohta, A. Takagi, T. Kamiya, M. Hirano, and H. Hosono, *Nature* **432**, 488 (2004).
- ¹³ T. Kamiya and H. Hosono, "Chap. 13 Amorphous In-Ga-Zn-O thin film transistors: fabrication and properties," in *Handbook of Zinc Oxide and Related Materials* (Taylor & Francis, 2012).
- ¹⁴ J. Kim, S. Watanabe, E. Matsuzaki, N. Nakamura, N. Miyakawa, Y. Toda, T. Kamiya, and H. Hosono, *SID Symposium Digest of Technical Papers* **46**, 1714 (2015).
- ¹⁵ S. Ueda, Y. Katsuya, M. Tanaka, H. Yoshikawa, Y. Yamashita, S. Ishimaru, Y. Matsushita, and K. Kobayashi, *AIP Conference Proceedings* **1234**, 403–406 (2010).
- ¹⁶ A. Layek, B. Yildirim, V. Ghodsi, L. Hutfluss, M. Hegde, T. Wang, and P. Radovanovic, *Chem. Mater.* **27**, 6030 (2015).
- ¹⁷ A. Szczesnak, T. Grzyb, Z. Sniadecki, N. Andrzejewska, S. Lis, M. Matczak, G. Nowaczyk, S. Jurga, and B. Idzikowski, *Inorg. Chem.* **53**, 12243 (2014).
- ¹⁸ T. Kamiya, K. Nomura, and H. Hosono, *J. Display Technol.* **5**, 273 (2009).
- ¹⁹ K. Ide, Y. Kikuchi, K. Nomura, M. Kimura, T. Kamiya, and H. Hosono, *Appl. Phys. Lett.* **99**, 093507 (2011).
- ²⁰ D. Li, X. Zhang, L. Jin, and D. Yang, *Opt. Exp.* **18**, 27191 (2010).
- ²¹ R. Cohen, G. Wertheim, A. Rosencwaig, and H. Guggenheim, *Phys. Rev. B* **5**, 1037 (1972).
- ²² C. Thiel, H. Cruguel, Y. Sun, G. Lapeyre, R. Macfarlane, R. Equall, and R. Cone, *J. Luminescence* **94**, 1 (2001).
- ²³ K. Yamamoto, K. Horiba, M. Taguchi, M. Matsunami, N. Kamakura, A. Chainani, Y. Takata, K. Mimura, M. Shiga, H. Wada, Y. Senba, H. Ohashi, and S. Shin, *Phys. Rev. B* **72**, 161101(R) (2005).
- ²⁴ E. Cho and S. Oh, *Phys. Rev. B* **59**, R15613 (1999).